An estimate of the longitudinal pace of aging from a single brain scan predicts dementia conversion, morbidity, and mortality

Ethan T. Whitman[1*], Maxwell L. Elliott[2*], Annchen R. Knodt[1], Wickliffe C. Abraham[3], Tim J. Anderson[4,5,6], Nick Cutfield[7], Sean Hogan[8], David Ireland[8], Tracy R. Melzer[9,10], Sandhya Ramrakha[8], Karen Sugden[1], Reremoana Theodore[8], Benjamin S. Williams[1], Avshalom Caspi[1,11,12,13,14], Terrie E. Moffitt[1,11,12,13,14], & Ahmad R. Hariri[1] for The Alzheimer's Disease Neuroimaging Initiative†

[1]Department of Psychology and Neuroscience, Duke University, Durham, NC, USA
[2]Department of Psychology, Center for Brain Science, Harvard University, Cambridge, MA, USA
[3]Department of Psychology, University of Otago, Dunedin, New Zealand
[4]Department of Medicine, University of Otago, Christchurch, New Zealand
[5]New Zealand Brain Research Institute, Christchurch, New Zealand
[6]Department of Neurology, Canterbury District Health Board, Christchurch, New Zealand
[7]Dunedin School of Medicine, University of Otago, Dunedin, New Zealand
[8]Dunedin Multidisciplinary Health and Development Research Unit, Department of Psychology, University of Otago, Dunedin, New Zealand
[9]Brain Research New Zealand-Rangahau Roro Aotearoa, Centre of Research Excellence, Universities of Auckland and Otago, New Zealand
[10]Department of Medicine, University of Otago, Christchurch, New Zealand
[11]Center for Genomic and Computational Biology, Duke University, Durham, NC, USA
[12]King's College London, Social, Genetic, and Developmental Psychiatry Centre, Institute of Psychiatry, Psychology, & Neuroscience, London, UK
[13]PROMENTA, Department of Psychology, University of Oslo, Norway
[14]Department of Psychiatry and Behavioral Sciences, Duke University, Durham, NC, USA

[*]These authors contributed equally to this work.

†Data used in preparation of this article were obtained from the Alzheimer's Disease Neuroimaging Initiative (ADNI) database (http://adni.loni.usc.edu). The investigators within ADNI contributed to the design and implementation of ADNI and/or provided data but did not participate in analysis or writing of this report. A complete listing of ADNI investigators can be found at: http://adni.loni.usc.edu/wp-content/uploads/how_to_apply/ADNI_Acknowledgement_List.pdf.

ABSTRACT

To understand how aging affects functional decline and increases disease risk, it is necessary to develop accurate and reliable measures of how fast a person is aging. Epigenetic clocks measure aging but require DNA methylation data, which many studies lack. Using data from the Dunedin Study, we introduce an accurate and reliable measure for the rate of longitudinal aging derived from cross-sectional brain MRI: the Dunedin Pace of Aging Calculated from NeuroImaging or DunedinPACNI. Exporting this measure to the Alzheimer's Disease Neuroimaging Initiative and UK Biobank neuroimaging datasets revealed that faster DunedinPACNI predicted participants' cognitive impairment, accelerated brain atrophy, and conversion to diagnosed dementia. Underscoring close links between longitudinal aging of the body and brain, faster DunedinPACNI also predicted physical frailty, poor health, future chronic diseases, and mortality in older adults. Furthermore, DunedinPACNI followed the expected socioeconomic health gradient. When compared to brain age gap, an existing MRI aging biomarker, DunedinPACNI was similarly or more strongly related to clinical outcomes. DunedinPACNI is a "next generation" MRI measure that will be made publicly available to the research community to help accelerate aging research and evaluate the effectiveness of dementia prevention and anti-aging strategies.

Aging is the gradual, progressive, and correlated decline of multiple organ systems over decades. Longitudinal studies provide evidence for substantial individual variation in the rate of aging; people born in the same year can age slower or faster than their peers[1–3]. Furthermore, aging itself is increasingly regarded as a potentially preventable cause of chronic disease. Accordingly, accurate and reliable measures of how fast a person is aging are needed to effectively study how individual variation in the rate of aging contributes to disease risk and to evaluate interventions intended to slow aging before irreversible decline[4–8].

Age-sensitive alterations in DNA methylation, referred to as "epigenetic clocks," are currently the most widely used measures for estimating individual differences in aging[4,9,10]. First-generation epigenetic clocks were trained on chronological age[11,12], but the more precisely they predicted chronological age, the less well they predicted clinical outcomes[13,14]. In response, second-generation clocks were trained on measures of health that predict mortality in older people[15–17]. However, these clocks were trained on cross-sectional phenotypes in multi-age samples, not on longitudinal observations of the same person as has been recommended in geroscience[5,18]. This limitation led to the development of a third-generation, longitudinal approach to measuring aging.

We previously adopted this longitudinal approach in the Dunedin Study, which has followed a population-representative sample of 1,037 people born in the same year (1972-1973) from birth to age 45[19]. Across two decades (ages 26, 32, 38, and 45 years), we repeatedly measured 19 biomarkers of cardiovascular, metabolic, renal, immune, dental, and pulmonary functioning. By averaging the decline in the trajectories of these biomarkers, we operationalized the theoretical construct of biological aging into a specific measure that we called the Pace of Aging[2]. We subsequently developed an epigenetic clock that accurately and reliably estimates the Pace of Aging: the Dunedin Pace of Aging Calculated from the Epigenome or DunedinPACE[20]. Because DunedinPACE is calculated from a single timepoint measurement of DNA methylation, it has been rapidly adopted by aging studies where it has been associated with signs of accelerated brain aging, morbidity, and mortality[20–25]. However, it has not been possible to export DunedinPACE or other epigenetic clocks to studies lacking DNA methylation data. This includes many neuroimaging studies of brain aging and neurodegenerative diseases such as Alzheimer's disease.

Current neuroimaging-based approaches to measure aging, akin to first-generation epigenetic clocks, involve training models to predict chronological age from variability in MRI measures of brain structure in large multi-age samples[26–30]. Researchers then typically quantify a "brain age gap," which reflects the difference between a participant's predicted and actual chronological age. A positive brain age gap is interpreted as evidence of accelerated brain aging. As with first-generation epigenetic clocks, these age-deviation approaches unavoidably mix model error (e.g., historical differences in environmental exposures, survivor bias, disease effects, measurement bias) with a person's true rate of biological aging[31–34].

Here, using a single T1-weighted MRI scan collected at age 45 in the Dunedin Study, we describe the development and validation of a novel brain MRI measure for the Pace of Aging (**Figure 1A-C**). We call this measure the Dunedin **P**ace of **A**ging **C**alculated from **N**euro**I**maging or "DunedinPACNI." Using data from the Human Connectome Project we evaluated the test-retest reliability of DunedinPACNI. Exporting the measure to the Alzheimer's Disease Neuroimaging Initiative (ADNI) and UK Biobank, we conducted a series of preregistered analyses (link: https://rb.gy/b9x4u6) designed to evaluate the utility of DunedinPACNI for predicting multiple aging-related health outcomes (**Figure 1D**). To benchmark our findings, we compared effect sizes for DunedinPACNI to those for brain age gap[35]. DunedinPACNI is the first brain-based measure trained to directly estimate longitudinal aging of non-brain organ systems. If

DunedinPACNI does indeed estimate individual differences in the rate of aging, it would add evidence for close links between brain integrity and whole-body aging and establish neuroimaging as a powerful tool for measuring aging; not just of the brain, but of the entire body[36].

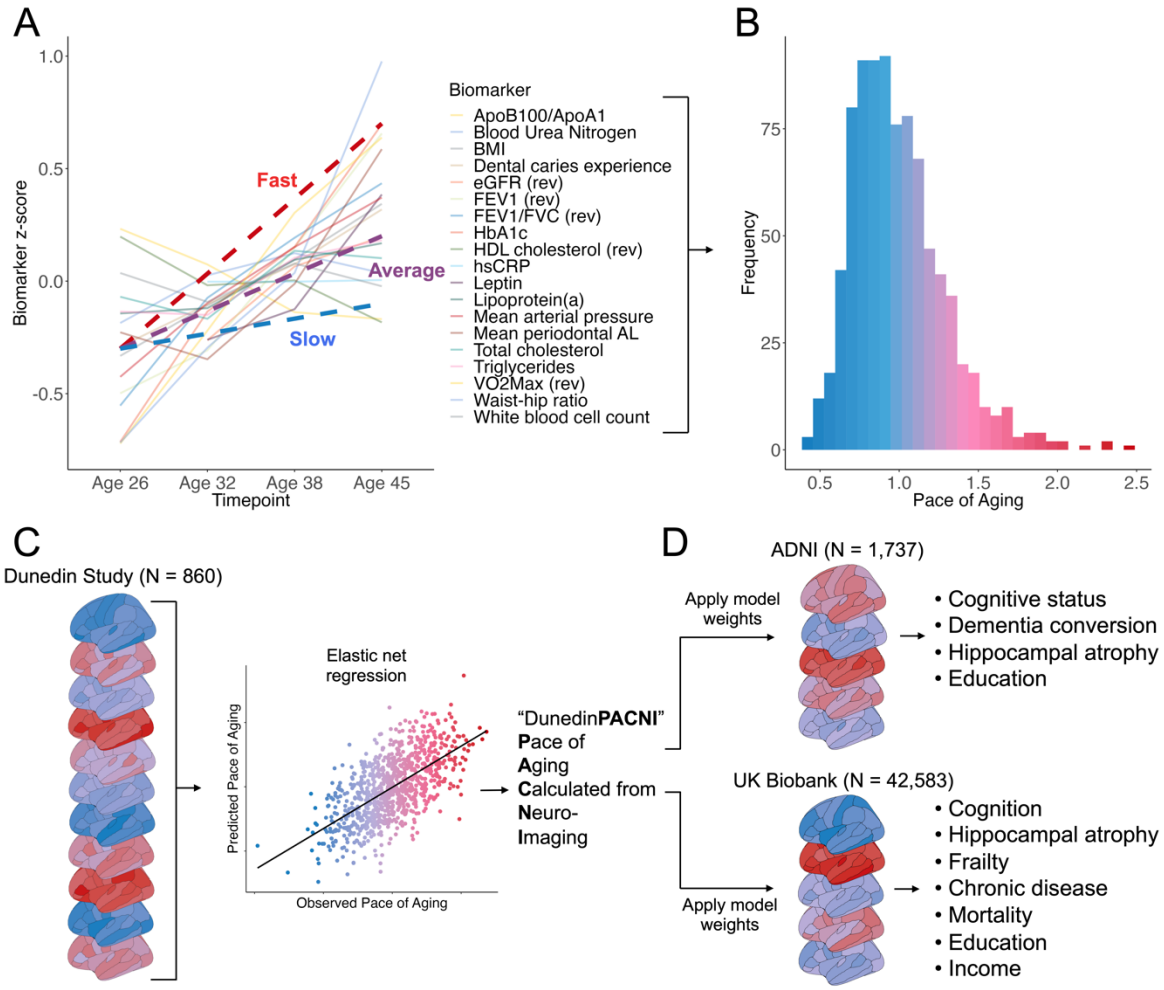

Figure 1. Schematic overview of study methods. A. Plot of mean scores for all 19 biomarkers comprising the Pace of Aging across four waves of observation at ages 26, 32, 38, and 45 years in the Dunedin Study. Hypothetical individual trajectories are shown for a person with relatively Slow, Average, and Fast Pace of Aging from ages 26 to 45. **B.** Distribution of Pace of Aging composite scores in Dunedin Study members at age 45. Warmer colors represent a faster Pace of Aging and cooler colors represent a slower Pace of Aging. **C.** A single T1-weighted MRI scan collected from 860 Dunedin Study members at age 45 was used to train an elastic net regression model to predict the Pace of Aging. We call the resulting measure the Dunedin Pace of Aging Calculated from NeuroImaging, or DunedinPACNI. **D.** Regression weights from the DunedinPACNI model developed in the Dunedin Study were applied to T1-weighted MRI scans collected in the Alzheimer's Disease Neuroimaging Initiative and UK Biobank datasets to derive DunedinPACNI scores. Those scores were then related to aging-related phenotypes. Abbreviations: ADNI = Alzheimer's Disease Neuroimaging Initiative.

RESULTS

DunedinPACNI: a Brain MRI Measure of Longitudinal Aging

We trained an elastic net regression model to predict the longitudinal Pace of Aging measure using T1-weighted MRI scans collected in a subsample of 860 Dunedin Study members when they were 45 years old. This subsample maintains the population-representativeness of the full cohort (see **Supplemental Figures S1-S2**). Specifically, the elastic net regression model used 315 MRI-derived structural measures for each Study member including regional cortical thickness, surface area, gray matter volume, and gray-white signal intensity ratio as well as subcortical gray matter and ventricular volumes[37]. We performed 10-fold cross-validation to identify optimal tuning parameters[38]. This optimized model was used to create DunedinPACNI.

The in-sample correlation between DunedinPACNI and the longitudinal Pace of Aging was r=0.60 (**Figure 2A**). We performed a cross-validation analysis by splitting the sample into training and testing subsets 100 different times. Each time, we used 90% of the sample for training and held out the remaining 10% for testing. Across all 100 different splits, the average correlation between DunedinPACNI and Pace of Aging in the testing sample was r=0.42. Of note, for both DunedinPACNI and the longitudinal Pace of Aging, higher scores indicate *faster* aging. Associations between faster DunedinPACNI scores and measures of physical functioning, cognitive functioning, and facial aging were similar to those previously observed with the Pace of Aging[2]. Specifically, DunedinPACNI effect sizes for 12 out of the 15 measures were within the 95% confidence intervals of the original Pace of Aging (**Figure 2B,** full results in **Supplemental Table S1**). This was expected given the high internal correlation between DunedinPACNI and Pace of Aging. Dunedin Study members with faster DunedinPACNI scores had worse balance, slower gait, weaker lower- and upper-body strength, and poorer coordination; they also reported worse health and more physical limitations; performed more poorly on tests of cognitive functioning; experienced greater childhood-to-adulthood cognitive decline; and looked older. These results indicate that DunedinPACNI accurately estimates the longitudinal Pace of Aging within the Dunedin Study dataset.

DunedinPACNI Reflects Canonical Patterns of Brain Aging

The optimized model used to derive DunedinPACNI included 99 regional brain measures. Due to difficulties in interpreting multivariable model coefficients, we used the Haufe transformation to estimate feature importance scores from the covariance between each brain measure and the Pace of Aging[39]. Given that many of the MRI-derived measures are highly correlated, our elastic net model reduced overfitting by setting the weights for many of them to 0 (visualized in **Supplemental Figure S3**). Faster Pace of Aging covaried with thinner cortex, smaller cortical surface area, smaller cortical gray matter volume, lower cortical gray-white intensity ratio, smaller subcortical gray matter volumes, and larger ventricular volumes (**Figure 2C**). We also observed positive covariance between calcarine cortical thickness and gray-white signal intensity ratio, though not calcarine gray matter volume. This is likely due to known aging-related effects on gray and white matter signal intensity that have been previously demonstrated[45–48]. These structural features overlap with the MRI signatures of both normal brain aging and neurodegenerative diseases[40–44], suggesting that faster DunedinPACNI reflects, at least in part, canonical patterns of brain aging.

DunedinPACNI has Excellent Test-Retest Reliability

If DunedinPACNI is to be used as a measure of aging, it must exhibit sufficient measurement reliability when exported to novel datasets. We used test-retest MRI data (N=45) from the Human Connectome Project[49] to estimate the reliability of DunedinPACNI. The test-retest reliability was excellent (ICC=0.94, 95% CI: [0.89-0.97], **Supplemental Figure S4**).

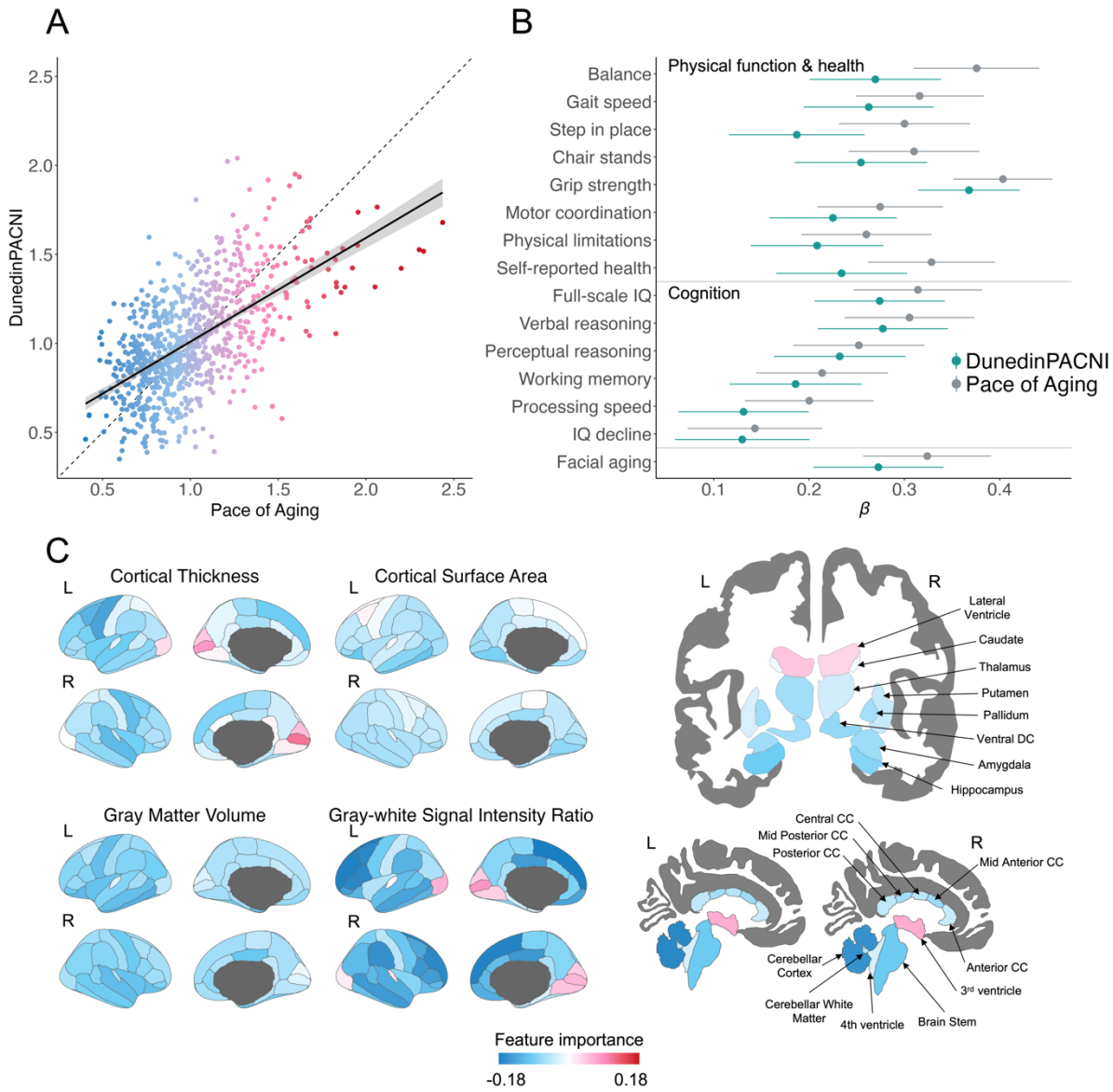

Figure 2. DunedinPACNI model validation and feature importance. A. In-sample correlation between Pace of Aging and DunedinPACNI. Warmer colors represent a faster Pace of Aging and cooler colors represent a slower Pace of Aging. **B.** Comparison of absolute effect sizes for associations between DunedinPACNI and Pace of Aging with physical functioning, cognition, and subjective aging measures within the Dunedin Study. Error bars represent the 95% confidence interval. **C.** Covariance between MRI-derived brain features and Pace of Aging. Of the 315 brain features used in model training, 216 were set equal to 0 due to the high correlation between brain measures in order to reduce overfitting. The 99 features included in the final model are visualized in **Supplemental Figure S3.** Warmer colors represent features that positively predicted DunedinPACNI scores (i.e., larger value indicates faster aging) while cooler colors represent features that negatively predicted DunedinPACNI scores (i.e., larger value indicates slower aging). Features that did not contribute to the accuracy of DunedinPACNI predictions are gray. Abbreviations: CC = corpus callosum, DC = diencephalon, L = left, R = right, IQ = Intelligence Quotient.

DunedinPACNI is Associated with Worse Cognitive Functioning

Having established both internal validity and test-retest reliability, we sought to examine whether DunedinPACNI generalizes to novel datasets to detect aging-related outcomes. Specifically, we first tested

for associations with cognitive functioning in ADNI and UK Biobank. We generated DunedinPACNI scores from T1-weighted MRI scans collected in 1,737 ADNI participants (mean age=74.3 SD=7.2; range: 52-97 years) and 42,583 UK Biobank participants (mean age=64.4, SD=7.7; range: 44-82 years). In ADNI, participants with faster DunedinPACNI performed worse on mental status exams used to screen for dementia as well as tests of memory, psychomotor speed, and executive functions; they also reported more impairment in cognitively demanding activities of daily living such as maintaining finances or preparing a meal (**Figure 3A**). Absolute standardized effect sizes across all cognitive measures in ADNI ranged from β=0.18 to 0.39 (all p-values<0.001, full results in **Supplemental Table S2**). Similarly, UK Biobank participants with faster DunedinPACNI performed more poorly on tests of executive functions and psychomotor speed (**Figure 3B**). Absolute standardized effect sizes across all cognitive measures in UK Biobank ranged from β=0.05 to 0.17 (all p-values<0.001, full results in **Supplemental Table S3**).

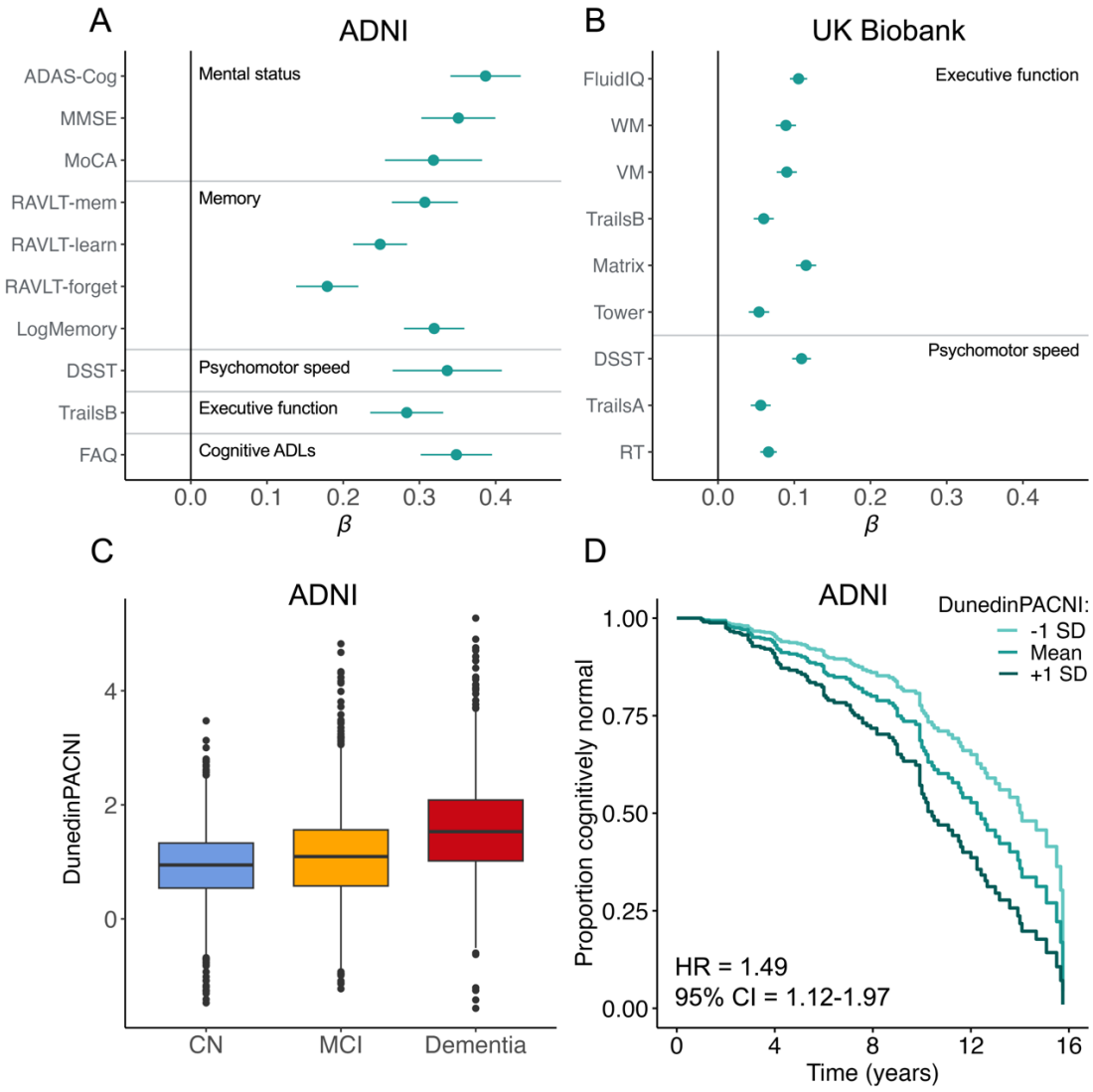

Figure 3. DunedinPACNI predicts cognition, cognitive impairment, and conversion to dementia. Cross-sectional associations between DunedinPACNI and cognitive test scores in **A.** ADNI and **B.** the UK Biobank. We visualize absolute effect sizes to aid visual comparison and clarity (see supplemental Tables S2 and S3 for raw effect sizes). Error bars represent the 95% confidence interval. **C**. Group differences in DunedinPACNI scores amongst ADNI

participants according to cognitive status at scanning. Center lines represent the median. Lower and upper hinges represent the 25th and 75th percentiles. Whiskers extend 1.5 times the inter-quartile range from the hinges. Data beyond the whiskers are plotted as individual outliers. **D**. Survival curve of the relative proportion of cognitively normal ADNI participants at baseline who remained cognitively normal during the follow-up window grouped by slow, average, and fast baseline DunedinPACNI scores. Abbreviations: ADAS-Cog = Alzheimer's Disease Assessment Scale – Cognitive Subscale 13, DSST = Digit Symbol Substitution Task, FAQ = Functional Activities Questionnaire, HR = hazard ratio, MMSE = Mini-Mental State Exam, MoCA = Montreal Cognitive Assessment, RT = Reaction Time, RAVLT = Rey Auditory Visual Learning Test, SD = standard deviation, Tower = Tower Rearranging, VM = Visual Memory, WM = Working Memory, CN = cognitively normal, MCI = mild cognitive impairment.

DunedinPACNI Predicts Cognitive Decline and Dementia Conversion

We next tested if DunedinPACNI differentiates between normal and clinically impaired cognitive functioning in ADNI (**Figure 3C**). Participants with mild cognitive impairment (MCI) had faster DunedinPACNI compared to cognitively normal participants (β=0.27, p<0.001, 95% CI: [0.18, 0.35]). Participants with dementia had faster DunedinPACNI than both participants with MCI (β=0.54, p<0.001, 95% CI: [0.43, 0.65] and cognitively normal participants (β=0.81 p<0.001, 95% CI: [0.69, 0.92]).

We further tested whether DunedinPACNI predicts future cognitive decline among people without cognitive impairment. Specifically, we analyzed a subsample of 624 ADNI participants who were cognitively normal at the time of their first scan, 112 of whom converted to either MCI or dementia during up to 16-years of follow-up. Cognitively normal participants with faster DunedinPACNI at baseline were more likely to develop MCI or dementia and to do so earlier during the follow-up window (HR=1.49, p=0.005, 95% CI: [1.12, 1.97]; **Figure 3D**), meaning those in the top 10% had a 61% increased risk of developing MCI or dementia compared to participants with average DunedinPACNI. We conducted a similar analysis among the 701 participants who were diagnosed with MCI at the time of their first scan, 271 of whom converted to dementia during the follow-up window. MCI participants with faster DunedinPACNI at baseline were more likely to convert to dementia (HR=1.44, p<0.001, 95% CI: [1.26, 1.65]). These effect sizes were similar when controlling for *APOE* ε4 allele carriership, a well-established genetic risk factor for sporadic, late-onset Alzheimer's disease (baseline cognitively normal: HR=1.49, p=0.005, 95% CI: [1.13, 1.96]; baseline MCI: HR=1.42, p<0.001, 95% CI: [1.23, 1.62]). Because only a very small number of UK Biobank participants with MRI data received diagnoses of dementia during follow-up observation (N=73), we were underpowered to report parallel results in this dataset.

DunedinPACNI Predicts Accelerated Brain Atrophy

As an estimate of how fast a person is aging, DunedinPACNI should reflect longitudinal trajectories of brain decline[33]. We tested whether faster baseline DunedinPACNI predicted accelerated hippocampal atrophy, which is an established risk factor for cognitive decline and dementia onset in older adults[50]. Specifically, we computed longitudinal trajectories of hippocampal atrophy among 1,302 ADNI participants who had MRI data at multiple time points (average number of scans=4.4, range=2 to 13 scans) as well as 4,628 UK Biobank participants who had MRI data at two timepoints. Participants with faster baseline DunedinPACNI exhibited accelerated hippocampal atrophy, in both ADNI (β=-0.15, p<0.001, 95% CI: [-0.21, -0.10]; **Figure 4B**) and the UK Biobank (β=-0.09, p<0.001, 95% CI: [-0.12, -0.05]; **Figure 4B**). This result was consistent while controlling for *APOE* ε4 allele carriership (**Supplemental Table S4**).

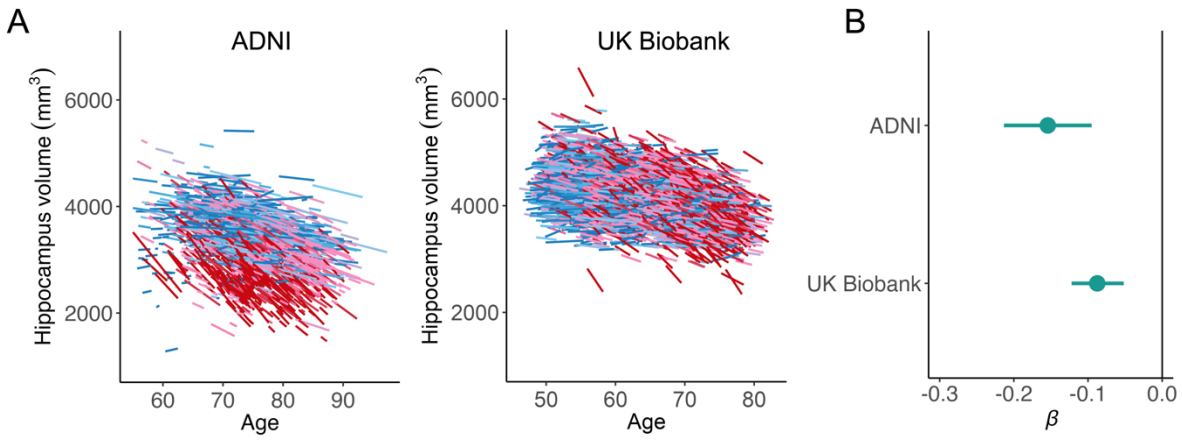

Figure 4. DunedinPACNI predicts accelerated hippocampal atrophy. A. Individualized trajectories of hippocampal atrophy in ADNI and UK Biobank. Warmer colors represent accelerated atrophy. **B.** Forest plot of associations between baseline DunedinPACNI scores and accelerated hippocampal atrophy in ADNI and UK Biobank. Error bars represent 95% confidence intervals and effect sizes. Abbreviations: mm^3 = cubic millimeters.

DunedinPACNI Predicts Frailty, Poor Health, Chronic Disease, and Mortality

As a measure of aging derived from longitudinal assessments of multiple biomarkers, DunedinPACNI should capture instances of declining health across all organ systems, not just the brain. To test this hypothesis, we used the UK Biobank to map DunedinPACNI scores onto measures of frailty, subjective overall health, incident aging-related chronic diseases, and all-cause mortality.

We used the Fried Frailty Index to quantify the degree of vulnerability to common stressors associated with aging-related decline in energy reserves and functioning. When treating index scores as a continuous measure ranging from 0 to 5 with higher scores indicating greater frailty[51,52], we found that participants with faster DunedinPACNI were more frail (N=42,583; β=0.17, p<0.001, 95% CI:[0.16, 0.18]). Participants with faster DunedinPACNI also self-reported poorer overall health (N=42,235; β=-0.17, p<0.001, 95% CI:[-0.18, -0.16]; **Figure 5A**), which predicts mortality even independently of objective health measures[53].

Similar patterns emerged when considering clinical diagnoses of chronic aging-related diseases including myocardial infarction, chronic obstructive pulmonary disease, dementia, and stroke. Participants with a lifetime prevalence of one of these chronic diseases had faster DunedinPACNI compared to those reporting no diagnoses (β=0.19, p<0.001, 95% CI: [0.16, 0.23]). Participants with a lifetime prevalence of two or more chronic diseases had faster DunedinPACNI than those with a single chronic disease (β=0.25, p<0.001, 95% CI: [0.12, 0.38] and those with no chronic disease (β=0.44, p<0.001, 95% CI: [0.31, 0.57]; **Figure 5B**).

Extending beyond contemporaneous associations, we assessed whether faster DunedinPACNI at baseline predicted future myocardial infarction, chronic obstructive pulmonary disease, dementia, or stroke in UK Biobank participants who were diagnosis-free at the time of scanning (N=40,753). 827 participants reported a new diagnosis of at least one of these aging-related chronic diseases over a maximum follow-up period of 9.7 years after scanning (i.e., baseline). Consistent with the above contemporaneous associations, healthy participants with faster DunedinPACNI at baseline were more likely to be later diagnosed with chronic aging-related diseases (HR=1.14, p<0.001, 95% CI: [1.05, 1.23]; **Figure 5C**), meaning those in the top 10% had an 18% or greater increased risk for developing a chronic disease compared to participants with average DunedinPACNI.

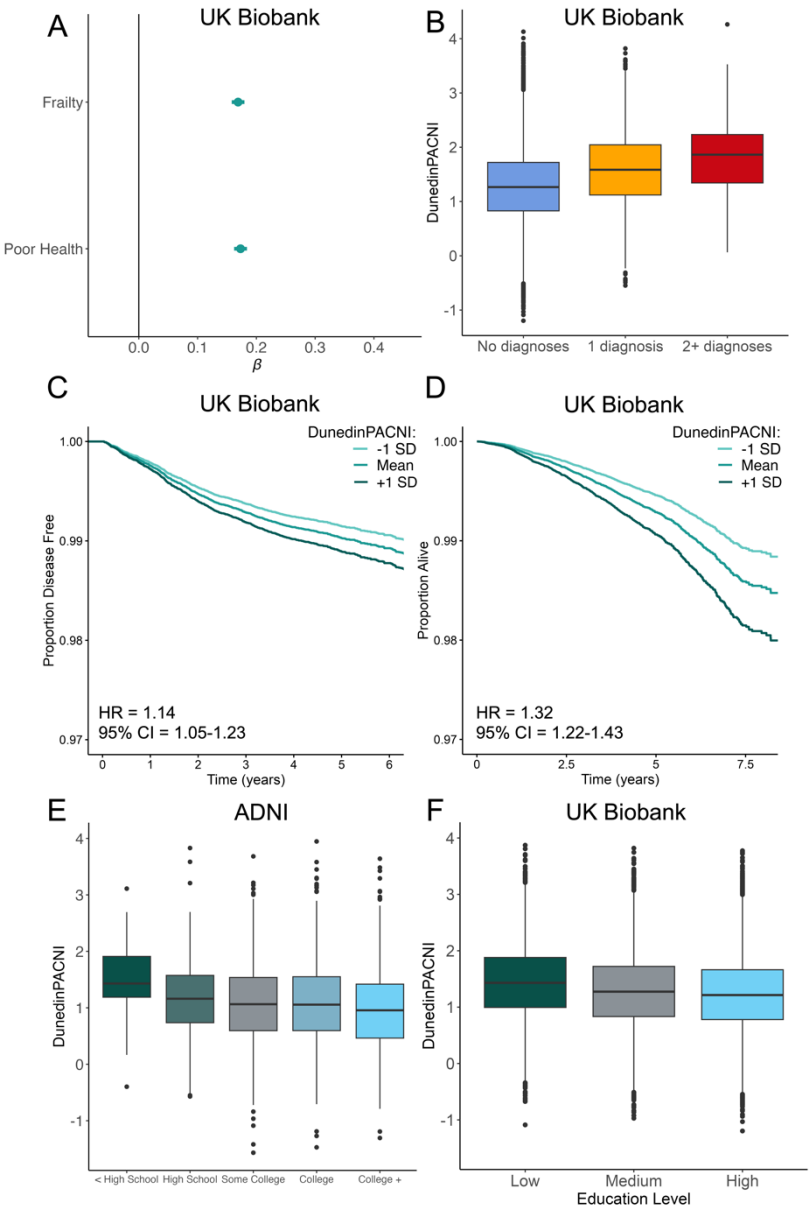

Figure 5. DunedinPACNI predicts frailty, poor health, multimorbidity, future chronic diseases, and mortality, and reflects social gradients of health inequities. A. Forest plot of absolute associations between DunedinPACNI and self-rated health and frailty in the UK Biobank. Error bars represent 95% confidence intervals. **B**. Group differences in DunedinPACNI scores according to lifetime number of aging-related chronic disease diagnoses including myocardial infarction, chronic obstructive pulmonary disease, dementia, and stroke in the UK Biobank. **C**. Survival curve of the relative proportion of disease-free UK Biobank participants at time of MRI who remained disease-free during the follow-up window, grouped by slow, average, and fast baseline DunedinPACNI scores. Of note, we excluded participants who had chronic disease prior to scanning from this analysis. **D.** Survival curve of the relative proportion of UK Biobank participants who remained alive during the follow-up window grouped by baseline DunedinPACNI scores. **E.** Group differences in DunedinPACNI according to education level among ADNI participants. **F.** Group differences in DunedinPACNI according to education level in the UK Biobank. For boxplots in **B**, **E**, and **F**, Center lines represent the median. Lower and upper hinges represent the 25th and 75th percentiles. Whiskers extend 1.5 times the inter-quartile range from the hinges. Data beyond the whiskers are plotted as individual outliers. Abbreviations: ADNI = Alzheimer's Disease Neuroimaging Initiative, HR = hazard ratio, SD = standard deviation.

Given the increased mortality rates amongst people with chronic aging-related diseases, we asked if baseline DunedinPACNI scores predicted all-cause mortality. Of the 42,583 UK Biobank participants included in our dataset, 757 died over the follow-up period after their baseline MRI scan. Participants with faster baseline DunedinPACNI scores died earlier (HR=1.32, p<0.001, 95% CI: [1.22, 1.43]; **Figure 5D**), meaning those in the top 10% were at least 41% more likely to die compared to participants with average DunedinPACNI. Taken together, these findings suggest that DunedinPACNI is useful for gauging general physical health and assessing risk for future chronic disease and death.

DunedinPACNI Reflects Social Gradients of Health Inequities

People who are less advantaged in their socioeconomic position experience a wide range of chronic diseases and earlier mortality[54–56], and DunedinPACNI should reflect such gradients of health inequities. We used information about educational attainment and income to test this prediction. Faster DunedinPACNI was observed for participants who either had fewer years of formal education (ADNI: β=-0.10, p<0.001, 95% CI: [-0.15, -0.05]; UK Biobank: β=-0.06, p<0.001, 95% CI: [-0.07, -0.05]) or lower income (UK Biobank: β=-0.09, p<0.001, 95% CI: [-0.10, -0.08]), reflecting the expected socioeconomic health gradient (**Figure 5E-F**).

DunedinPACNI is Distinct from Brain Age Gap

Lastly, we compared DunedinPACNI with existing age-deviation approaches for measuring aging using brain MRI data. Specifically, we compared effect sizes for DunedinPACNI from all of the aforementioned analyses in ADNI and UK Biobank with brain age gap generated using brainageR[35]. We selected this algorithm due to its high accuracy and test-retest reliability compared to other brain age gap algorithms[57]. Compared to brain age gap, the effect sizes for DunedinPACNI were similar or larger across measures of cognitive function, cognitive decline, brain atrophy, frailty, disease risk, mortality, and socioeconomic health gradients (**Figure 6,** full results in **Supplemental Tables S2-S3, S5-S8**). DunedinPACNI and brain age gap were only modestly correlated (ADNI: r=0.17, p <0.001; UK Biobank: r=0.31, p<0.001; **Supplemental Figure S5**). Commensurate with this low correlation, when we included both DunedinPACNI and brain age gap in a single model, each measure explained unique variance in clinical outcomes with only minor reductions in effect sizes. Moreover, using both DunedinPACNI and brain age gap together in a single model generally increased prediction of these outcomes (**Supplemental Figure S6**). For example, the combined hazard ratio of DunedinPACNI and brain age gap predicting mortality risk was 1.50 (95% CI: [1.36, 1.65]), compared to the independent hazard ratios of 1.32 for DunedinPACNI and 1.24 for brain age gap.

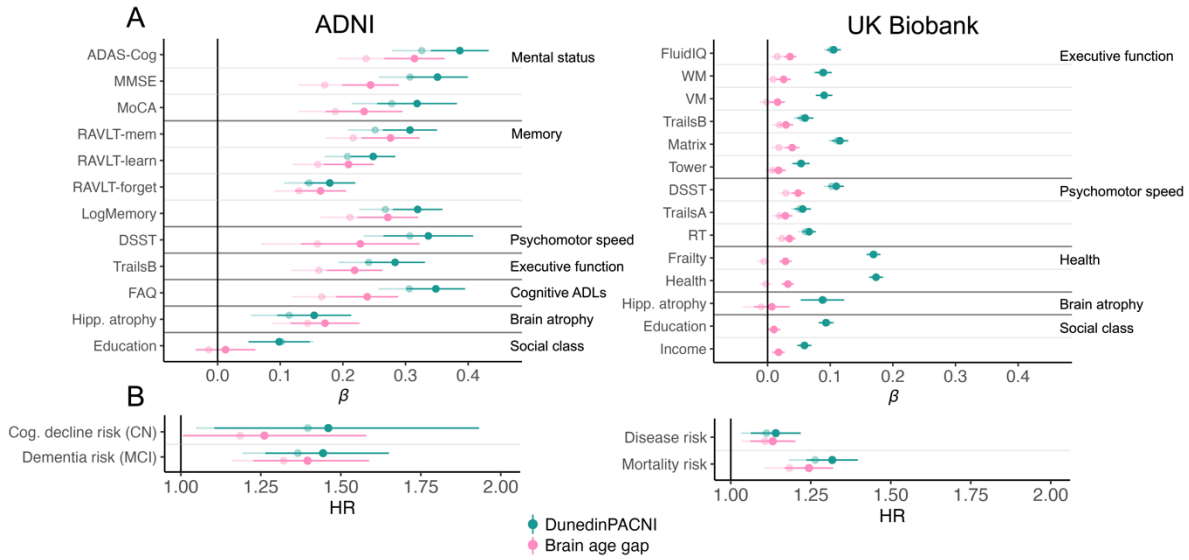

Figure 6. Comparison of DunedinPACNI and brain age gap associations with aging-related phenotypes. A. Forest plots of DunedinPACNI and brain age gap absolute effect sizes in ADNI and UK Biobank. **B.** Forest plots of DunedinPACNI and brain age gap hazard ratios in ADNI and UK Biobank. Error bars represent 95% confidence intervals. Lighter shades represent the effect size for each measure while controlling for the other measure (i.e., effect of DunedinPACNI when controlling for brain age gap, and vice versa). Abbreviations: ADAS-Cog = Alzheimer's Disease Assessment Scale – Cognitive Subscale 13, CN = cognitively normal, DSST = Digit Symbol Substitution Task, FAQ = Functional Activities Questionnaire, HR = hazard ratio, Hipp. = hippocampus, MCI = mild cognitive impairment, MMSE = Mini-Mental State Exam, MoCA = Montreal Cognitive Assessment, RT = Reaction Time, RAVLT = Rey Auditory Visual Learning Test, Tower = Tower Rearranging, VM = Visual Memory, WM = Working Memory.

DISCUSSION

DunedinPACNI is an accurate and reliable measure of how fast a person is aging derived from a single brain MRI scan. Using data from ADNI and UK Biobank, we demonstrate that people with faster DunedinPACNI had not only worse cognitive and brain health (i.e., poorer cognition, faster hippocampal atrophy, and greater dementia risk) but also worse general health (i.e., greater frailty, poorer self-reported health, greater risk of chronic disease and mortality). Across all analyses, the effect sizes for DunedinPACNI were similar or larger than the effect sizes for brain age gap, an existing age-deviation measure derived from the same structural MRI data. Moreover, DunedinPACNI and brain age gap were only weakly correlated, and DunedinPACNI accounted for incremental variance in aging-related health outcomes. While weak correlations between neuroimaging-based measures of aging may appear surprising, they mirror findings that different epigenetic clocks are also weakly correlated, and multiple clocks are useful for predicting disease and death[58,59]. Aging remains a construct in search of measurement tools[4,5], and DunedinPACNI represents a "next-generation" measure of aging that is distinct from existing approaches.

DunedinPACNI is not without limitations. First, the Dunedin Study, ADNI, and UK Biobank consist of data collected primarily from participants of European ancestry. Furthermore, ADNI and UK Biobank may over sample participants from higher socioeconomic backgrounds[60]. Neuroimaging-based predictive models sometimes perform poorly when tested on people who demographically differ from the training sample (e.g., low socioeconomic status and non-White people)[61]. More generally, there is a growing awareness of the need for improved representativeness in neuroimaging research[62,63]. Notably, we found that

associations with DunedinPACNI were consistent when tested among low-income or non-White participants in the UK Biobank (**Supplemental Tables S9-S10**). The findings in ADNI and UK Biobank demonstrate that the predictive utility of DunedinPACNI generalizes to older adults. A priority for future work is to further evaluate the generalizability of DunedinPACNI to older adults from different ethnic and socioeconomic backgrounds. Second, DunedinPACNI only uses structural brain measures derived from a T1-weighted MRI scan. We chose this strategy because these scans are collected in nearly every MRI study, thereby maximizing the potential adoption of DunedinPACNI. It is possible that the performance accuracy reported here could be improved by including additional structural and/or functional MRI measures (e.g., white matter microstructural integrity from diffusion weighted images, BOLD signal from T2*-weighted images). Third, by design, DunedinPACNI is a measure of the longitudinal rate of the aging of the body derived from a single MRI scan and is not designed to replace longitudinal measurement of brain aging through repeated MRI assessments. Fourth, DunedinPACNI is estimated through observed correlations between measures of brain structure and longitudinal aging, which could reflect multiple causal pathways. For example, faster aging of non-brain organs might cause poorer brain health or vice versa. Alternatively, both may be driven by a third factor. Fifth, although we found robust associations with aging phenotypes across both ADNI and UK Biobank, we generally observed larger effect sizes in ADNI. This could suggest that DunedinPACNI is especially sensitive to dysfunction among patients with neurodegenerative diseases. Further evaluation is needed to establish the degree to which DunedinPACNI is sensitive to individual organ systems.

Several unique features of the Dunedin Study contribute advantages to DunedinPACNI compared to other aging biomarkers. First, DunedinPACNI was developed in a cohort of people all born in the same year and studied at the same ages throughout their lives, thereby avoiding biases that are introduced by differences in historical exposures across generations and across time. Second, DunedinPACNI is trained on 19 biomarkers that were each assessed over two decades and thus is not influenced by short-term illnesses that can cause aberrant biomarker signals at a single assessment. Third, DunedinPACNI was derived from participants followed from birth to age 45 before the onset of chronic, aging-related diseases that cause divergence from typical trajectories of aging. Fourth, because the Dunedin Study cohort is population-representative with very low attrition and mortality rates, DunedinPACNI does not suffer from oversampling of healthy volunteers, attrition bias (i.e., people with worse health being more likely to drop out), or survivor bias (i.e., people with worse health dying earlier). Indeed, our results align with prior research showing that DunedinPACE, which like DunedinPACNI was trained on the longitudinal Pace of Aging, is associated with dementia, morbidity, and mortality[20,22,23]. Our results, alongside the fast-growing literature on DunedinPACE, suggest that these unique design characteristics of the Dunedin Study make it a powerful training sample for longitudinal aging biomarkers.

The scope of geroscience has rapidly expanded with the proliferation of -omic clocks that can measure how fast people age[10]. DunedinPACNI is poised to further this growth by allowing individual differences in the rate of longitudinal aging to be estimated from a single noninvasive MRI scan that can be collected in just a few minutes. Indeed, the requisite MRI data to estimate DunedinPACNI have already been collected in many psychiatric, neurologic, and brain-health cohorts, from tens of thousands of research participants across the lifespan and around the world. DunedinPACNI offers an opportunity to enrich such studies and deepen understanding of the causes of individual differences in the rate of longitudinal aging, including genetics[64], childhood adversities[65], environmental exposures (e.g., lead[66,67]), and lifestyle factors (e.g., physical inactivity, social isolation[68]). DunedinPACNI may also be adopted as a surrogate endpoint to accelerate our ability to develop, prioritize, and evaluate potential anti-aging interventions that slow aging and prevent disease[69,70]. The algorithm for DunedinPACNI will be made publicly available to the research community to facilitate these and other future research directions.

METHODS

The premise and analysis plan for this study were pre-registered (link: https://rb.gy/b9x4u6). All analyses and code were checked for accuracy by an independent analyst. Analyses were conducted on data collected through the Dunedin Study, Human Connectome Project, Alzheimer's Disease Neuroimaging Initiative, and UK Biobank. Details for each study and dataset are described below.

DATA SOURCES

Dunedin Study

Participants are members of the Dunedin Study, a longitudinal investigation of health and behavior in a representative birth cohort. The 1,037 participants (91% of eligible births, 48% female) were all people born between April 1972 and March 1973 in Dunedin, New Zealand, who were residents in the province and who participated in the first assessment at age 3 years[19]. The cohort represented the full range of socioeconomic status in the general population of New Zealand's South Island and, as adults, matches the New Zealand National Health and Nutrition Survey on key adult health indicators (e.g., body mass index, smoking, and general practitioner visits) and the New Zealand Census of citizens of the same age on educational attainment[19,71]. The overall cohort is primarily New Zealand European/White (7.5% self-identifying as Māori).

General assessments were performed at birth as well as ages 3, 5, 7, 9, 11, 13, 15, 18, 21, 26, 32, and 38 years; and, most recently (completed April 2019), at age 45 years, when 938 of the 997 living Study members (94.1%) participated. At each assessment, Study members were brought to the Dunedin Study Research Unit at the University of Otago for interviews and examinations. In addition, staff provided standardized ratings, informant questionnaires were sent to people who the Study members nominated as people who knew them well, and administrative records were searched. The Dunedin Study was approved by the University of Otago Ethics Committee and Study members gave written informed consent before participating.

MRI

As a component of the age 45 assessments, Study members were scanned using a Siemens MAGNETOM Skyra (Siemens Healthcare GmbH) 3T scanner equipped with a 64-channel head/neck coil at the Pacific Radiology Group imaging center in Dunedin, New Zealand. High resolution T1-weighted images were obtained using an MP-RAGE sequence with the following parameters: TR=2400 ms; TE=1.98 ms; 208 sagittal slices; flip angle, 9°; FOV, 224 mm; matrix =256×256; slice thickness=0.9 mm with no gap (voxel size 0.9×0.875×0.875 mm); and total scan time=6 min and 52 s. 3D fluid-attenuated inversion recovery (FLAIR) images were obtained with the following parameters: TR=8000 ms; TE=399 ms; 160 sagittal slices; FOV=240 mm; matrix=232×256; slice thickness=1.2 mm (voxel size 0.9×0.9×1.2 mm); and total scan time=5 min and 38 s. Additionally, a gradient-echo field map was acquired with the following parameters: TR=712 ms; TE=4.92 and 7.38 ms; 72 axial slices; FOV=200 mm; matrix=100×100; slice thickness=2.0 mm (voxel size 2 mm isotropic); and total scan time=2 min and 25 s. Of the 938 Study members seen at Phase 45, 63 declined to participate in MRI scanning, meaning 875 Study members completed the MRI scanning protocol. Scanned Study members did not differ significantly from other living participants in terms of childhood neurocognitive functioning or childhood SES (see attrition analysis in the **Supplemental Figures S1-S2**). Of these 875 Study members for whom data was available, 4 were excluded due to major incidental findings or previous injuries (e.g. large tumors or extensive damage to the brain/skull), 9 due to missing FLAIR or field map scans, 1 due to poor surface mapping yielding, and 1 due to missing the Pace of Aging variable. This yielded a final training sample of 860 Study members (see **Supplemental Figure S7** for inclusion details).

Structural MRI data were analyzed using the Human Connectome Project (HCP) minimal preprocessing pipeline as detailed elsewhere[72]. Briefly, T1-weighted and FLAIR images were processed through the PreFreeSurfer, FreeSurfer, and PostFreeSurfer pipelines. T1-weighted and FLAIR images were corrected for readout distortion using the gradient echo field map, coregistered, brain-extracted, and aligned together in the native T1 space using boundary-based registration[73]. Images were then processed with a custom FreeSurfer recon-all pipeline that is optimized for structural MRI with a higher resolution than 1 mm isotropic.

Pace of Aging

Participants' pace of biological aging was measured as changes in 19 biomarkers of cohort members' cardiovascular, metabolic, pulmonary, kidney, immune and dental systems across ages 26, 32, 38, and 45 years. This measure quantifies participants' rate of aging in year-equivalent units of physiological decline per chronological year. The average participant experienced 1 year of physiological decline per year, a mean (SD) Pace of Aging of 1 (0.3)[2] . See the Statistical Analysis section for more details.

Physical Functioning

One-legged balance was measured using the Unipedal Stance Test as the maximum time achieved across three trials of the test with eyes closed[76–78]. Gait speed (meters per second) was assessed with the 6-m-long GAITRite Electronic Walkway (CIR Systems, Inc) with 2-m acceleration and 2-m deceleration before and after the walkway, respectively. Gait speed was assessed under 3 walking conditions: usual gait speed (walk at a normal pace from a standing start, measured as a mean of 2 walks) and 2 challenge paradigms, dual-task gait speed (walk at a normal pace while reciting alternate letters of the alphabet out loud, starting with the letter "A," measured as a mean of 2 walks) and maximum gait speed (walk as fast as safely possible, measured as a mean of 3 walks). Gait speed was correlated across the 3 walk conditions[75]. To increase reliability and take advantage of the variation in all 3 walk conditions (usual gait and the 2 challenge paradigms), we calculated the mean of the 3 highly correlated individual walk conditions to generate our primary measure of composite gait speed. The step in place test was measured as the number of times the right knee was lifted to mid-thigh height (measured as the height half-way between the knee cap and the iliac crest) in 2 minutes at a self-directed pace[80]. Chair rises were measured as the number of stands with no hands completed in 30 seconds from a seated position[79]. Handgrip strength was measured for each hand (elbow held at 90°, upper arm held tight against the trunk) as the maximum value achieved across three trials using a Jamar digital dynamometer[80,81]. Analyses using handgrip strength controlled for BMI. Visual-motor coordination was measured as the time to completion of the Grooved Pegboard Test. Scores were reversed so that higher values corresponded to better performance. Physical limitations were measured with the RAND 36-Item Health Survey 1.0 physical functioning scale. Responses ("limited a lot", "limited a little", "not limited at all") assessed difficulty with completing various activities (e.g., climbing several flights of stairs, walking more than 1 km, participating in strenuous sports). Scores were reversed to reflect physical limitations so that a high score indicates more limitations.

Subjective Health and age appearance

We obtained reports about Study members' health and age appearance from three sources: self-reports, informant impressions, and staff impressions. We obtained reports about Study members' age appearance from three sources: self-reports, informant impressions, and staff impressions. *Self-reports* – We asked the Study members about their own impressions of how old they looked, "Do you think you LOOK older, younger, or about your actual age?" Response options were younger than their age, about their actual age, or older than their age. We also asked Study members to rate their age perceptions in years, "How old do you feel?" *Informant impressions* - Informants who knew a Study member well (94%

response rate) were asked: "Compared to others their age, do you think he/she (the Study member) looks younger or older than others their age? Response options were: "much younger", "a bit younger", "about the same", "a bit older", or "much older". *Staff impressions* - Four members of the Dunedin Study Unit staff completed a brief questionnaire describing each study member. To assess age appearance, staff used a 7-item scale to assign a "relative age" to each Study member (1=young looking, 7=old looking). Correlations between self-, informant-, and staff-ratings ranged from 0.34–0.52. All reporters rated the Study member's general health using the following response options: excellent, very good, good, fair, or poor. Correlations between self-, informant-, and staff-ratings ranged from *r=0*.48–0.55.

Cognitive Functioning

The Wechsler Adult Intelligence Scale-IV (WAIS-IV) was administered at age 45, yielding adult IQ. In addition to full-scale IQ, the WAIS-IV yields indexes of four specific cognitive function domains: Processing Speed, Working Memory, Perceptual Reasoning, and Verbal Comprehension. The Wechsler Intelligence Scale for Children–Revised (WISC–R) was administered at ages 7, 9, and 11 years. To increase baseline reliability the three scores were averaged yielding childhood IQ. We measured cognitive decline by studying adult IQ scores after controlling for childhood IQ scores. We focus on change in overall IQ given evidence that aging-related slopes are correlated across all cognitive functions, indicating that research on cognitive decline may be best focused on a highly reliable summary index, rather than focused on individual functions[74].

Facial Age

Facial Age was based on two measurements of perceived age by an independent panel of eight people. First, age range was assessed by an independent panel of four raters, who were presented with standardized (non-smiling) digital facial photographs of Study members when they were 45 years old. Raters, who were kept blind to the actual age of Study members, used a Likert scale to categorize each Study member into a 5-year age range (i.e., from 20–24 years old up to 70+ years old). Interrater reliability was 0.77. Scores for each Study member were averaged across all raters. Second, relative age was assessed by a different panel of four raters, who were told that all photos were of people aged 45 years old. These raters then used a 7-item Likert scale to assign a "relative age" to each participant (i.e., 1 = "young looking," to 7 = "old looking"). Interrater reliability was 0.79. The measure of perceived age at 45 years (i.e., Facial Age) was derived by standardizing and averaging age range and relative age scores.

Human Connectome Project (HCP)

The HCP is a publicly available dataset that includes 1,206 participants with extensive MRI data[49]. HCP data access is managed by the WU-Minn HCP consortium. All participants provided informed consent. Specifically, we used data from 45 participants who completed the scan protocol a second time (with a mean interval between scans of approximately 140 days) allowing for calculation of test-retest reliability. All participants were free of current psychiatric or neurologic illness and were between 25 and 35 years of age.

MRI

Structural MRI data were analyzed using the Human Connectome Project minimal preprocessing pipeline[72]. Briefly, T1-weighted images were processed using a custom FreeSurfer recon-all pipeline that is optimized for structural MRI with a higher resolution than 1 mm isotropic. Details on HCP MRI data acquisition have been described elsewhere[72].

Alzheimer's Disease Neuroimaging Initiative (ADNI)

The primary goal of ADNI is to test whether serial MRI, PET, other biological markers, and clinical and neuropsychological assessments can be combined to measure the progression of neurodegeneration in participants with mild cognitive impairment, Alzheimer's disease, and cognitively normal older adults (adni.loni.usc.edu)[82]. For further information, see adni.loni.usc.edu. Cognitive and diagnostic data were downloaded on June 12th, 2022. MRI data curated from the Alzheimer's Disease Sequencing Project (ADSP) collection were downloaded on December 7th, 2023. ADNI was approved by the Institutional Review Boards of all the participating institutions. All participants provided written informed consent. ADNI sample demographic information can be found in **Supplemental Table S11.**

MRI

T1-weighted scans were collected using either 1.5T or 3T scanners. MRI acquisition parameters varied across ADNI sites and waves; however, the targets for acquisition were isotropic $1mm^3$ voxels.[83]. Raw T1-weighted images were processed using longitudinal FreeSurfer version 6.0. Scans were excluded for low quality if they did not have a QC rating of 'Pass' from ADNI investigators or if segmentation failed visual inspection. Scans were also excluded if participants were missing demographic data such as age, sex, or diagnosis (**Supplemental Figure S8)**. Further details on MRI methods in ADNI can be found at adni.loni.usc.edu.

Cognitive and Behavioral Functioning

ADNI participants completed several cognitive and behavioral assessments at the time of scanning. The Alzheimer's Disease Assessment Scale – Cognitive Subscale 13 (ADAS-Cog) is a structured scale that evaluates memory, reasoning, language, orientation, ideational praxis, and constructional praxis[84]. Delayed Word Recall and Number Cancellation are included in addition to the 11 standard ADAS Items[85]. The test is scored for errors, ranging from 0 (best performance) to 85 (worst performance). The Mini Mental State Exam (MMSE) is a screening instrument that evaluates orientation, memory, attention, concentration, naming, repetition, comprehension, and ability to create a sentence and to copy 2 overlapping pentagons[86]. The MMSE is scored as the number of correctly completed items ranging from 0 (worst performance) to 30 (best performance). The Montreal Cognitive Assessment (MoCA) is designed to detect people at the MCI stage of cognitive dysfunction[87]. The scale ranges from 0 (worst performance) to 30 (best performance). The Rey Auditory Verbal Learning Test is a list learning task which assesses learning and memory. On each of 5 learning trials, 15 unrelated nouns are presented orally at the rate of 1 word per second and immediate free recall of the words is elicited. After a 30-minute delay filled with unrelated testing, free recall of the original 15-word list is elicited. Both immediate recall and the percent forgotten are used. The Logical Memory tests I and II (Delayed Paragraph Recall) is from the Wechsler Memory Scale–Revised. Free recall of 1 short story is elicited immediately after being read aloud to the participant and again after a 30-minute delay. The total bits of information recalled after the delay interval (maximum score = 25) are analyzed. The Trail Making Test, Part B, consists of 25 circles, either numbered (1 through 13) or containing letters (A through L). Participants connect the circles while alternating between numbers and letters (e.g., A to 1; 1 to B; B to 2; 2 to C). Time to complete (300 seconds maximum) is the primary measure of interest. The Functional Assessment Questionnaire (FAQ) is a self-report measure of instrumental activities of daily living such as preparing meals, performing chores, keeping a schedule, and traveling outside of one's neighborhood[88]. Each unique cognitive testing measure was paired with the participant's most temporally proximate brain scan within 6 months of cognitive testing.

Cognitive Status

ADNI participants were classified into cognitively normal (CN), mild cognitive impairment (MCI), or dementia groups by ADNI study physicians based on subjective memory complaints, multiple neurocognitive and behavioral assessment scores, and level of impairment in activities of daily living.

Complete diagnostic criteria can be found at adni.loni.usc.edu. Each individual scan was categorized according to the most temporally proximate cognitive diagnosis received by that participant.

Education

Education level was measured according to self-reported years of education. For the purposes of visualization in **Figure 5E**, participants were grouped according to the following thresholds: Less than high school: < 12 years; High school: 12 years; Some college: 12-15 years; College: 16 years; More than college: >16 years.

UK Biobank

The UK Biobank is a United Kingdom population-based prospective study of 502,486 participants between the ages of 40 and 69 at baseline assessment[89]. We analyzed data from 42,583 participants who underwent brain MRI. Data used in these analyses were downloaded in April 2023. The UK Biobank was approved by the North West Multi-centre for Research Ethics Committee. All participants provided written informed consent. UK Biobank sample demographic information can be found in **Supplemental Table S11**.

MRI

MRI methods for the UK Biobank have been described in detail elsewhere[90]. Briefly, MRI data were collected using 3 identical 3T Siemens Skyra scanners with a 32-channel Siemens head coil. T1-weighted images were obtained using a 3D MP-RAGE with the following parameters: TR = 2000 ms; TI = 880 ms; 208 sagittal slices, matrix =256×256; slice thickness = 1 mm with no gap; and total scan time = 4 min and 52 s. Our study made use of imaging-derived phenotypes generated by an image-processing pipeline developed and run on behalf of the UK Biobank[90]. As part of this pipeline, raw T1-weighted images were processed using the cross-sectional FreeSurfer version 6.0. All brain measures used in the cross-sectional analyses presented here were derived from the outputs of this FreeSurfer pipeline. We excluded UK Biobank participants with very low signal-to-noise ratio and highly unusual summary morphometrics indicative of low-quality reconstruction **(Supplemental Figure S9).**

To analyze the longitudinal UK Biobank MRI data, we reprocessed all T1-weighted images using the longitudinal FreeSurfer version 6.0 pipeline[91]. This allowed us to avoid the known biases that can be introduced by different processing stages of the longitudinal pipeline on different hardware and software environments. Specifically, we reprocessed both time points of each participant's T1-weighted scans with the cross-sectional recon-all pipeline[92]. Then we built an unbiased within-subject template[93] using robust, inverse consistent registration[94] and reprocessed each T1-weighted scan through the automated longitudinal pipeline[91].

Cognitive Functioning

UK Biobank participants completed a battery of cognitive tests at the time of MRI. We investigated cognitive functioning using the following measures: Reaction Time (Field ID = 20023), Fluid Intelligence (Field ID = 20016), Numeric Memory (Field ID = 4282), Trails A (Field ID = 6348) and B (Field ID = 6350), Symbol Digit Substitution (Field ID = 23324), Tower Rearranging (Field ID = 21004), and Matrix Completion (Field ID = 6373). The details of these cognitive tests have been described elsewhere[95].

Frailty and Self-Reported Health

To further investigate aging-related health, we used the Fried Frailty Index[52]. Briefly, the Fried Frailty Index is based on meeting criteria for declining functioning across five domains: unintentional weight loss, exhaustion, weakness, physical inactivity, and slow walking speed. Index scores range from 0 to 5 with

higher scores indicating greater frailty[96]. During their imaging visit, UK Biobank participants were also asked to rate their overall health as "Poor," "Fair," "Good," or "Excellent." We used these ratings to investigate self-reported overall health (Field ID = 4548).

Disease and Mortality Records

To assess the influence of DunedinPACNI on aging-related disease and mortality risk in UK Biobank we used variables from algorithmically defined health outcomes. Briefly, algorithmically defined outcomes are generated by combining information from baseline assessments (self-reported medical conditions, operations, and medications) with linked data from hospital admissions and death registries. Due to the relatively small number of aging-related disease diagnoses at follow-up, we defined aging-related morbidity as being diagnosed with myocardial infarction (Field ID = 42000), chronic obstructive pulmonary disease (Field ID = 42016), dementia (Field ID = 42018), or stroke (Field ID = 42006). Furthermore, we defined risk of chronic disease as the emergence or one or more of these diagnoses among participants who were healthy at the time of scanning (i.e., baseline). Mortality was quantified during follow-up from death records (Field ID = 40000).

Education, Income, and Ethnicity

To test the association between DunedinPACNI and socioeconomic gradients of health, we tested whether UK Biobank participants differed in DunedinPACNI scores as a function of educational attainment and household income. We grouped participants into three categories according to their self-reported educational qualifications (Field ID = 6138) following prior work[97]. Specifically, these groups were: high (college or university degree), medium (A/AS levels or equivalent or O/levels/GCSEs or equivalent), and low (none of these). We also tested whether UK Biobank participants differed in DunedinPACNI scores as a function of household income (Field ID = 738).

We also conducted sensitivity analyses while restricting the UK Biobank sample to either only low income or only non-White participants. We considered participants low income if they reported making < £18,000 per year in household income. We considered participants to be non-White if they did not report their ethnic background (Field ID = 21000) as "Any other white background," "British," "Do not know," "Irish," "Prefer not to answer," or "White."

STATISTICAL ANALYSES

Pace of Aging

The derivation of the Pace of Aging has been described elsewhere[1,2]. Briefly, we measured a panel of the following 19 biomarkers (**Figure 1A**) at ages 26, 32, 38, and 45: body mass index (BMI), waist-hip ratio, glycated hemoglobin, leptin, blood pressure (mean arterial pressure), cardiorespiratory fitness (VO_2max), forced vital capacity ratio (FEV_1/FVC), forced expiratory volume in one second (FEV_1), total cholesterol, triglycerides, high-density lipoprotein (HDL), lipoprotein(a), apolipoprotein B100/A1 ratio, estimated glomerular filtration rate (eGFR), blood urea nitrogen (BUN), high sensitivity C-reactive protein (hs-CRP), white blood cell count, mean periodontal attachment loss (AL), and the number of dental-caries-affected tooth surfaces (tooth decay). To calculate each Study members Pace of Aging, we first transformed the biomarker values to a standardized scale. For each biomarker at each wave, we standardized values according to the age-26 distribution. Next, we calculated each Study member's slope for each of the 19 biomarkers using a mixed-effects growth model that regressed the biomarker's level on age. Finally, we combined information from the 19 slopes of the biomarkers using a unit-weighting scheme. We calculated each Study member's Pace of Aging as the sum of age-dependent annual changes in biomarker Z-scores. Biomarker standardization was performed separately for men and women.

DunedinPACNI

A schematic of DunedinPACNI model development can be found in **Figure 1**. We trained an elastic net regression model to estimate the Pace of Aging from structural neuroimaging phenotypes in 860 Dunedin Study members at age 45 (for attrition analysis and inclusion criteria see **Supplemental Figures S1-S2, S7**). We selected 315 variables as predictors from the following categories: regional cortical thickness (CT), regional cortical surface area (SA), regional cortical gray matter volume (GMV), regional cortical gray-white matter signal intensity ratio (GWR), and 'ASEG' volumes (i.e., regional subcortical gray matter volumes, ventricular volumes, and bilateral volume of white matter hypointensities). All cortical data were parcellated according to the Desikan-Killainy Atlas[98]. Four phenotypes from the 'ASEG' volumes were excluded due to insufficient variance in the Dunedin Study (left and right white matter hypointensities, left and right non-white matter hypointensities). Model training was performed using the *caret* package in R. We conducted a grid search across a range of α and λ values. We used 100 repetitions of 10-fold cross-validation to estimate model performance in held-out participants. The effect of sex was regressed from the Pace of Aging prior to model training. To prevent information leak during cross-validation, we regressed sex from each training set and applied the resulting beta weights to each test set. This approach ensured that our model only used information from the training set, including covariate regression, when calculating predictions in each test set. We selected optimal tuning parameters according to highest variance explained and lowest mean absolute error. The optimal tuning parameters were α = 0.214 and λ = 0.100. Using these parameters, we fit the model to the entire N=860 sample. The raw elastic net regression model weights can be found in **Supplemental Table S12**.

To generate DunedinPACNI scores in HCP, ADNI, and UK Biobank participants, we applied the regression weights from the DunedinPACNI model to FreeSurfer-derived phenotypes within each dataset and summed the products and model intercept. In ADNI and UK Biobank, DunedinPACNI scores were correlated with chronological age (ADNI: r=0.37; UK Biobank: r=0.50; **Supplemental Figure S10**).

In addition, we conducted the same procedure again without GWR as this measure is not always distributed in public datasets. We observed slightly reduced model accuracy when GWR was not included. DunedinPACNI estimates without GWR phenotypes showed excellent test re-test reliability in HCP. DunedinPACNI estimates were similar with and without GWR phenotypes in ADNI and UK Biobank (see **Supplemental Figure S11** for more details).

Brain Age Gap

We submitted raw T1-weighted images from ADNI and UK Biobank to the publicly available brainageR algorithm. This model, which has been described in detail elsewhere[99], was selected because it generates the most reliable estimates amongst published algorithms[57]. Briefly, brainageR is estimated by first segmenting and normalizing T1-weighted images using SPM12. Next, coefficients derived from a Gaussian Process regression model predicting chronological age in a training dataset (N=2,001) are applied to morphometric features from brain segmentations to predict participants' chronological age. Brain age gap was subsequently estimated by subtracting actual chronological age from predicted age[99]. Of note, 15 scans failed the brain age gap pipeline (14 failed visual inspection of segmentation, 1 error computing predicted age). These scans were excluded from all brain age gap analyses, including comparative analyses with DunedinPACNI.

Dunedin Study Validation Analyses

To first test the validity of DunedinPACNI within the Dunedin Study training sample, we tested for linear associations between DunedinPACNI scores and one-legged balance, gait speed, step in place, chair

stands, grip strength, visual-motor coordination, subjective physical limitations, subjective health, cognitive function, child-to-adult cognitive decline, and facial aging while controlling for sex. We compared these effect sizes to associations between each of these measures and the original, 20-year Pace of Aging.

Test-Retest Reliability

We used the HCP dataset to assess the test-retest reliability of DunedinPACNI. Reliability was quantified using a two-way mixed-effects ICC (3,1) with session modeled as a fixed effect, subject as a random effect, and test-retest interval as an effect of no interest[100].

Cognitive and Physical Functioning

We first used linear regression models to test for associations between DunedinPACNI and scores on tests of cognition, physical function, and health in ADNI and UK Biobank. All analyses controlled for age and sex. In ADNI, we calculated robust standard errors to account for non-independence from repeated observations. In addition, we conducted a sensitivity analysis while controlling for *APOE* ε4 carriership, which conveys genetic risk for AD. We also tested the standardized differences in DunedinPACNI scores between three groups based on cognitive status: cognitively normal (CN), mild cognitive impairment (MCI), and dementia. All group difference comparisons controlled for age and sex. We again calculated robust standard errors to account for non-independence and conduced a sensitivity analysis while controlling for *APOE* ε4 carriership. We repeated these analyses with brain age gap. Of note, when conducting analyses on the combined effects of DunedinPACNI and brain age gap on cognitive outcomes in ADNI, we restricted the sample to the first timepoint of each measure. This included only one observation per participant, allowing us to more easily combine effect sizes and confidence intervals.

Dementia Survival Analysis

We conducted a Cox-proportional hazard regression using ADNI participants' baseline DunedinPACNI scores to predict their probability of cognitive decline or clinically conversion to dementia during the follow-up window. Conversion among cognitively normal participants was defined as having a diagnosis of CN at baseline but a diagnosis of MCI or dementia at the end of follow-up. Conversion among MCI participants was defined as having a diagnosis of MCI at baseline and a diagnosis of dementia by the end of follow-up. Participants who had a baseline diagnosis of dementia or transitioned from MCI to CN were not included in this analysis. The analysis controlled for sex, age at baseline, and length of observation window. We investigated the influence of AD genetic risk on these results by conducting all analyses while additionally controlling for *APOE* ε4 carriership. We repeated these analyses for brain age gap.

Prediction of Hippocampal Atrophy Rates

We used repeated MRI measurements from the ADNI (N = 1,302) and UK Biobank (N = 4,628) to generate estimates of change in hippocampal gray matter volume. We ran longitudinal ComBat on ADNI MRI data to remove differential scanner effects[101]. Next, using all available timepoints for each participant, we generated multilevel linear models for bilateral hippocampal volume with random effects for both participant and age. Using these models, we derived trajectories to track change in hippocampal gray matter volume for each participant. We then tested whether each participant's baseline DunedinPACNI scores could predict their subsequent rate of hippocampal atrophy. These analyses controlled for age, sex, and length of observation period. We investigated the influence of AD genetic risk on these results by conducting these analyses while additionally controlling for *APOE* ε4 carriership. We repeated these analyses for brain age gap.

Morbidity and Mortality Survival Analyses

To investigate the association between DunedinPACNI and morbidity, we used UK Biobank data to calculate the standardized differences in DunedinPACNI scores between three groups based on number of lifetime chronic disease diagnosis (0, 1, 2+). Next, we conducted a Cox-proportional hazard regression using UK Biobank participants' baseline DunedinPACNI scores to predict the onset of a chronic aging-related disease (N=827 emergent diagnoses: myocardial infarction, chronic obstructive pulmonary disease, dementia, or stroke) in participants who had never previously received any of these diagnoses at the time of scanning (N=40,753). Similarly, to investigate the association between DunedinPACNI and mortality we conducted a Cox-proportional hazard regression using UK Biobank participants' baseline DunedinPACNI scores to predict death (N=757 deaths). Both models controlled for baseline age, time to onset, and sex. We repeated these analyses for brain age gap.

Socioeconomic Inequality Analyses

To investigate whether DunedinPACNI reflected gradients of socioeconomic inequality[56], we first tested for linear relationships between DunedinPACNI and years of education in ADNI and UK Biobank. We also tested for a linear relationship between DunedinPACNI and household income in UK Biobank. These analyses controlled for sex and age. In ADNI, we included only the first MRI observation per participant.

REFERENCES

1. Belsky, D. W. *et al.* Quantification of biological aging in young adults. *Proc. Natl. Acad. Sci. U. S. A.* **112**, (2015).
2. Elliott, M. L. *et al.* Disparities in the pace of biological aging among midlife adults of the same chronological age have implications for future frailty risk and policy. *Nat. Aging* **1**, 295–308 (2021).
3. Kuo, P.-L. *et al.* Longitudinal phenotypic aging metrics in the Baltimore Longitudinal Study of Aging. *Nat. Aging* **2**, 635–643 (2022).
4. Moqri, M. *et al.* Biomarkers of aging for the identification and evaluation of longevity interventions. *Cell* **186**, 3758–3775 (2023).
5. Moqri, M. *et al.* Validation of biomarkers of aging. *Nat. Med.* **30**, 360–372 (2024).
6. Justice, J. N. & Kritchevsky, S. B. Putting epigenetic biomarkers to the test for clinical trials. *Elife* **9**, (2020).
7. Melton, L. Scientists hone tools to measure aging and rejuvenation interventions. *Nat. Biotechnol.* **41**, 1359–1361 (2023).
8. Ubaida-Mohien, C. *et al.* Blood biomarkers for healthy aging. *Gerontology* **69**, 1167–1174 (2023).
9. Horvath, S. & Raj, K. DNA methylation-based biomarkers and the epigenetic clock theory of ageing. *Nat. Rev. Genet.* **19**, 371–384 (2018).
10. Rutledge, J., Oh, H. & Wyss-Coray, T. Measuring biological age using omics data. *Nat. Rev. Genet.* **23**, 715–727 (2022).
11. Hannum, G. *et al.* Genome-wide methylation profiles reveal quantitative views of human aging rates. *Mol. Cell* **49**, 359–367 (2013).
12. Horvath, S. DNA methylation age of human tissues and cell types. *Genome Biology* **14**, R115 (2013).
13. Zhang, Q. *et al.* Improved precision of epigenetic clock estimates across tissues and its implication for biological ageing. *Genome Med.* **11**, (2019).
14. Raffington, L. & Belsky, D. W. Integrating DNA methylation measures of biological aging into social determinants of health research. *Curr. Environ. Health Rep.* **9**, 196–210 (2022).
15. Lu, A. T. *et al.* DNA methylation GrimAge strongly predicts lifespan and healthspan. *Aging (Albany NY)* **11**, 303–327 (2019).
16. Levine, M. E. *et al.* An epigenetic biomarker of aging for lifespan and healthspan. *Aging (Albany NY)* **10**, 573–591 (2018).
17. Sehgal, R. *et al.* Systems Age: A single blood methylation test to quantify aging heterogeneity across 11 physiological systems. *bioRxiv* 2023.07.13.548904 (2023) doi:10.1101/2023.07.13.548904.
18. Moffitt, T. E. Behavioral and social research to accelerate the geroscience translation agenda. *Ageing Res. Rev.* **63**, 101146 (2020).
19. Poulton, R., Guiney, H., Ramrakha, S. & Moffitt, T. E. The Dunedin study after half a century: reflections on the past, and course for the future. *J. R. Soc. N. Z.* **53**, 446–465 (2023).
20. Belsky, D. W. *et al.* DunedinPACE, a DNA methylation biomarker of the pace of aging. *Elife* **11**, (2022).
21. Whitman, E. T. *et al.* A blood biomarker of the pace of aging is associated with brain structure: replication across three cohorts. *Neurobiol. Aging* **136**, 23–33 (2024).
22. Sugden, K. *et al.* Association of pace of aging measured by blood-based DNA methylation with age-related cognitive impairment and dementia. *Neurology* **99**, e1402–e1413 (2022).
23. Faul, J. D. *et al.* Epigenetic-based age acceleration in a representative sample of older Americans: Associations with aging-related morbidity and mortality. *Proc. Natl. Acad. Sci. U. S. A.* **120**, e2215840120 (2023).
24. Harris, K. M. *et al.* The sociodemographic and lifestyle correlates of epigenetic aging in a nationally representative U.s. study of younger adults. *bioRxiv* 2024.03.21.585983 (2024) doi:10.1101/2024.03.21.585983.

25. Guida, J. L. *et al.* Associations of seven measures of biological age acceleration with frailty and all-cause mortality among adult survivors of childhood cancer in the St. Jude Lifetime Cohort. *Nat. Cancer* 1–11 (2024).
26. Cole, J. H. *et al.* Predicting brain age with deep learning from raw imaging data results in a reliable and heritable biomarker. *Neuroimage* **163**, 115–124 (2017).
27. Bashyam, V. M. *et al.* MRI signatures of brain age and disease over the lifespan based on a deep brain network and 14 468 individuals worldwide. *Brain* **143**, 2312–2324 (2020).
28. Yin, C. *et al.* Anatomically interpretable deep learning of brain age captures domain-specific cognitive impairment. *Proc. Natl. Acad. Sci. U. S. A.* **120**, (2023).
29. Korbmacher, M. *et al.* Brain asymmetries from mid- to late life and hemispheric brain age. *Nat. Commun.* **15**, 1–14 (2024).
30. Han, L. K. M. *et al.* Brain aging in major depressive disorder: results from the ENIGMA major depressive disorder working group. *Mol. Psychiatry* **26**, 5124–5139 (2021).
31. Sluiskes, M. H. *et al.* Clarifying the biological and statistical assumptions of cross-sectional biological age predictors: an elaborate illustration using synthetic and real data. *BMC Med. Res. Methodol.* **24**, (2024).
32. Butler, E. R. *et al.* Pitfalls in brain age analyses. *Hum. Brain Mapp.* **42**, 4092–4101 (2021).
33. Vidal-Pineiro, D. *et al.* Individual variations in 'brain age' relate to early-life factors more than to longitudinal brain change. *Elife* **10**, e69995 (2021).
34. Sluiskes, M. H. *et al.* Clarifying the biological and statistical assumptions of cross-sectional biological age predictors. *bioRxiv* (2023) doi:10.1101/2023.01.01.522413.
35. Biondo, F. *et al.* Brain-age is associated with progression to dementia in memory clinic patients. *NeuroImage Clin.* **36**, 103175 (2022).
36. Brain and body are more intertwined than we knew. *Nature* **623**, 223–224 (2023).
37. Fischl, B. FreeSurfer. *Neuroimage* **62**, 774–781 (2012).
38. Hsu, C.-W., Chang, C.-C. & Lin, C.-J. A practical guide to support vector classification. https://www.csie.ntu.edu.tw/~cjlin/papers/guide/guide.pdf.
39. Haufe, S. *et al.* On the interpretation of weight vectors of linear models in multivariate neuroimaging. *Neuroimage* **87**, 96–110 (2014).
40. Raz, N. *et al.* Regional brain changes in aging healthy adults: General trends, individual differences and modifiers. *Cereb. Cortex* **15**, 1676–1689 (2005).
41. Salat, D. H. Thinning of the cerebral cortex in aging. *Cereb. Cortex* **14**, 721–730 (2004).
42. Planche, V. *et al.* Structural progression of Alzheimer's disease over decades: the MRI staging scheme. *Brain Commun.* **4**, fcac109 (2022).
43. Salat, D. H. *et al.* Age-associated alterations in cortical gray and white matter signal intensity and gray to white matter contrast. *Neuroimage* **48**, 21–28 (2009).
44. Walhovd, K. B. *et al.* Effects of age on volumes of cortex, white matter and subcortical structures. *Neurobiol. Aging* **26**, 1261–1270 (2005).
45. Vidal-Piñeiro, D. *et al.* Accelerated longitudinal gray/white matter contrast decline in aging in lightly myelinated cortical regions. *Hum. Brain Mapp.* **37**, 3669–3684 (2016).
46. Grydeland, H., Walhovd, K. B., Tamnes, C. K., Westlye, L. T. & Fjell, A. M. Intracortical myelin links with performance variability across the human lifespan: Results from T1- and T2-weighted MRI myelin mapping and diffusion tensor imaging. *J. Neurosci.* **33**, 18618–18630 (2013).
47. Storsve, A. B. *et al.* Differential longitudinal changes in cortical thickness, surface area and volume across the adult life span: Regions of accelerating and decelerating change. *J. Neurosci.* **34**, 8488–8498 (2014).
48. Natu, V. S. *et al.* Apparent thinning of human visual cortex during childhood is associated with myelination. *Proc. Natl. Acad. Sci. U. S. A.* **116**, 20750–20759 (2019).

49. Van Essen, D. C. *et al.* The WU-Minn Human Connectome Project: An overview. *Neuroimage* **80**, 62–79 (2013).
50. Jack, C. R., Jr *et al.* Rates of hippocampal atrophy correlate with change in clinical status in aging and AD. *Neurology* **55**, 484–489 (2000).
51. Jiang, R. *et al.* Associations of physical frailty with health outcomes and brain structure in 483 033 middle-aged and older adults: a population-based study from the UK Biobank. *Lancet Digit. Health* **5**, e350–e359 (2023).
52. Fried, L. P. *et al.* Frailty in older adults: Evidence for a phenotype. *J. Gerontol. A Biol. Sci. Med. Sci.* **56**, M146–M157 (2001).
53. Idler, E. L. & Benyamini, Y. Self-rated health and mortality: a review of twenty-seven community studies. *J. Health Soc. Behav.* **38**, 21–37 (1997).
54. Chen-Xu, J. *et al.* Subnational inequalities in years of life lost and associations with socioeconomic factors in pre-pandemic Europe, 2009–19: an ecological study. *Lancet Public Health* **9**, e166–e177 (2024).
55. Balaj, M. *et al.* Parental education and inequalities in child mortality: a global systematic review and meta-analysis. *Lancet* **398**, 608–620 (2021).
56. Marmot, M. G. *et al.* Health inequalities among British civil servants: the Whitehall II study. *Lancet* **337**, 1387–1393 (1991).
57. Dörfel, R. P. *et al.* Prediction of brain age using structural magnetic resonance imaging: A comparison of accuracy and test–retest reliability of publicly available software packages. *Hum. Brain Mapp.* **44**, 6139–6148 (2023).
58. Belsky, D. W. *et al.* Eleven telomere, epigenetic clock, and biomarker-composite quantifications of biological aging: Do they measure the same thing? *Am. J. Epidemiol.* (2017) doi:10.1093/aje/kwx346.
59. Moqri, M. *et al.* A unified framework for systematic curation and evaluation of aging biomarkers. *Research Square* (2024) doi:10.21203/rs.3.rs-4481437/v1.
60. Brayne, C. & Moffitt, T. E. The limitations of large-scale volunteer databases to address inequalities and global challenges in health and aging. *Nat. Aging* **2**, 775–783 (2022).
61. Greene, A. S. *et al.* Brain–phenotype models fail for individuals who defy sample stereotypes. *Nature* **609**, 109–118 (2022).
62. Wig, G. S. *et al.* Participant diversity is necessary to advance brain aging research. *Trends Cogn. Sci.* **28**, 92–96 (2024).
63. Falk, E. B. *et al.* What is a representative brain? Neuroscience meets population science. *Proc. Natl. Acad. Sci. U. S. A.* **110**, 17615–17622 (2013).
64. Melzer, D., Pilling, L. C. & Ferrucci, L. The genetics of human ageing. *Nat. Rev. Genet.* **21**, 88–101 (2020).
65. Kim, K. *et al.* Association of adverse childhood experiences with accelerated epigenetic aging in midlife. *JAMA Netw. Open* **6**, e2317987 (2023).
66. Reuben, A. *et al.* Association of childhood lead exposure with MRI measurements of structural brain integrity in midlife. *JAMA* **324**, 1970 (2020).
67. Lee, H., Lee, M. W., Warren, J. R. & Ferrie, J. Childhood lead exposure is associated with lower cognitive functioning at older ages. *Sci. Adv.* **8**, (2022).
68. Livingston, G. *et al.* Dementia prevention, intervention, and care: 2020 report of the Lancet Commission. *Lancet* **396**, 413–446 (2020).
69. Barzilai, N., Crandall, J. P., Kritchevsky, S. B. & Espeland, M. A. Metformin as a tool to target aging. *Cell Metab.* **23**, 1060–1065 (2016).
70. Kraus, W. E. *et al.* 2 years of calorie restriction and cardiometabolic risk (CALERIE): exploratory outcomes of a multicentre, phase 2, randomised controlled trial. *Lancet Diabetes Endocrinol.* **7**, 673–683 (2019).

71. Richmond-Rakerd, L. S. *et al.* Clustering of health, crime and social-welfare inequality in 4 million citizens from two nations. *Nat. Hum. Behav.* **4**, 255–264 (2020).
72. Glasser, M. F. *et al.* The minimal preprocessing pipelines for the Human Connectome Project. *Neuroimage* **80**, 105–124 (2013).
73. Greve, D. N. & Fischl, B. Accurate and robust brain image alignment using boundary-based registration. *Neuroimage* **48**, 63–72 (2009).
74. Tucker-Drob, E. M., Brandmaier, A. M. & Lindenberger, U. Coupled cognitive changes in adulthood: A meta-analysis. *Psychol. Bull.* **145**, 273–301 (2019).
75. Rasmussen, L. J. H. *et al.* Association of neurocognitive and physical function with gait speed in midlife. *JAMA Netw. Open* **2**, e1913123 (2019).
76. Bohannon, R. W., Larkin, P. A., Cook, A. C., Gear, J. & Singer, J. Decrease in timed balance test scores with aging. *Phys. Ther.* **64**, 1067–1070 (1984).
77. Vereeck, L., Wuyts, F., Truijen, S. & Van de Heyning, P. Clinical assessment of balance: normative data, and gender and age effects. *Int. J. Audiol.* **47**, 67–75 (2008).
78. Springer, B. A., Marin, R., Cyhan, T., Roberts, H. & Gill, N. W. Normative values for the unipedal stance test with eyes open and closed. *J. Geriatr. Phys. Ther.* **30**, 8–15 (2007).
79. Jones, C. J., Rikli, R. E. & Beam, W. C. A 30-s chair-stand test as a measure of lower body strength in community-residing older adults. *Res. Q. Exerc. Sport* **70**, 113–119 (1999).
80. Mathiowetz, V. *et al.* Grip and pinch strength: normative data for adults. *Arch. Phys. Med. Rehabil.* **66**, 69–74 (1985).
81. Rantanen, T. *et al.* Midlife hand grip strength as a predictor of old age disability. *JAMA* **281**, 558–560 (1999).
82. Veitch, D. P. *et al.* The Alzheimer's Disease Neuroimaging Initiative in the era of Alzheimer's disease treatment: A review of ADNI studies from 2021 to 2022. *Alzheimers. Dement.* **20**, 652–694 (2024).
83. Jack, C. R., Jr *et al.* The Alzheimer's Disease Neuroimaging Initiative (ADNI): MRI methods. *J. Magn. Reson. Imaging* **27**, 685–691 (2008).
84. Rosen, W. G., Mohs, R. C. & Davis, K. L. A new rating scale for Alzheimer's disease. *Am. J. Psychiatry* **141**, 1356–1364 (1984).
85. Mohs, R. C. *et al.* Development of cognitive instruments for use in clinical trials of antidementia drugs: additions to the Alzheimer's Disease Assessment Scale that broaden its scope. The Alzheimer's Disease Cooperative Study. *Alzheimer Dis. Assoc. Disord.* **11 Suppl 2**, S13-21 (1997).
86. Folstein, M. F., Folstein, S. E. & McHugh, P. R. "Mini-mental state". A practical method for grading the cognitive state of patients for the clinician. *J. Psychiatr. Res.* **12**, 189–198 (1975).
87. Nasreddine, Z. S. *et al.* The Montreal Cognitive Assessment, MoCA: a brief screening tool for mild cognitive impairment. *J. Am. Geriatr. Soc.* **53**, 695–699 (2005).
88. Pfeffer, R. I., Kurosaki, T. T., Harrah, C. H., Jr, Chance, J. M. & Filos, S. Measurement of functional activities in older adults in the community. *J. Gerontol.* **37**, 323–329 (1982).
89. Sudlow, C. *et al.* UK biobank: an open access resource for identifying the causes of a wide range of complex diseases of middle and old age. *PLoS Med.* **12**, e1001779 (2015).
90. Alfaro-Almagro, F. *et al.* Image processing and Quality Control for the first 10,000 brain imaging datasets from UK Biobank. *Neuroimage* **166**, 400–424 (2018).
91. Reuter, M., Schmansky, N. J., Rosas, H. D. & Fischl, B. Within-subject template estimation for unbiased longitudinal image analysis. *Neuroimage* **61**, 1402–1418 (2012).
92. Fischl, B. & Dale, A. M. Measuring the thickness of the human cerebral cortex from magnetic resonance images. *Proc. Natl. Acad. Sci. U. S. A.* **97**, 11050–11055 (2000).
93. Reuter, M. & Fischl, B. Avoiding asymmetry-induced bias in longitudinal image processing. *Neuroimage* **57**, 19–21 (2011).

94. Reuter, M., Rosas, H. D. & Fischl, B. Highly accurate inverse consistent registration: a robust approach. *Neuroimage* **53**, 1181–1196 (2010).
95. Fawns-Ritchie, C. & Deary, I. J. Reliability and validity of the UK Biobank cognitive tests. *PLoS One* **15**, e0231627 (2020).
96. Williams, D. M., Jylhävä, J., Pedersen, N. L. & Hägg, S. A frailty index for UK biobank participants. *J. Gerontol. A Biol. Sci. Med. Sci.* **74**, 582–587 (2019).
97. Chadeau-Hyam, M. *et al.* Education, biological ageing, all-cause and cause-specific mortality and morbidity: UK biobank cohort study. *EClinicalMedicine* **29–30**, 100658 (2020).
98. Desikan, R. S. *et al.* An automated labeling system for subdividing the human cerebral cortex on MRI scans into gyral based regions of interest. *Neuroimage* **31**, 968–980 (2006).
99. Cole, J. H. *et al.* Brain age predicts mortality. *Mol. Psychiatry* **23**, 1385–1392 (2018).
100. Shrout, P. E. & Fleiss, J. L. Intraclass correlations: uses in assessing rater reliability. *Psychol. Bull.* **86**, 420–428 (1979).
101. Beer, J. C. *et al.* Longitudinal ComBat: A method for harmonizing longitudinal multi-scanner imaging data. *Neuroimage* **220**, 117129 (2020).

DATA AVAILABILITY

Dunedin Study data is available via managed access at https://sites.duke.edu/moffittcaspiprojects/data-use-guidelines/. The Human Connectome Project data are publicly available at http://www.humanconnectomeproject.org/data/. Alzheimer's Disease Neuroimaging Initiative data are publicly available at https://adni.loni.usc.edu/. Researchers can apply to access all UK Biobank data at https://ams.ukbiobank.ac.uk/ams/.

CODE AVAILABILITY

The DunedinPACNI algorithm will be made available for download upon publication. All scripts used in the analyses presented here are available at https://github.com/etw11/WhitmanElliott_2024.

ACKNOWLEDGEMENTS

This research received support from the US National Institute on Aging (grants R01AG049789, R01AG032282, R01AG073207) and the UK Medical Research Council (grant MR/X021149/1). The Dunedin Multidisciplinary Health and Development Research Unit is supported by the New Zealand Health Research Council (Programme Grant 16-604).

We thank the Dunedin Study members, Unit research staff, previous Study Director, Emeritus Distinguished Professor, the late Richie Poulton, for his leadership during the Study's research transition from young adulthood to aging (2000-2023), and Study founder Dr Phil A. Silva. The Dunedin Unit is located within the Ngāi Tahu tribal area who we acknowledge as first peoples, tangata whenua (people of this land).

This research has been conducted using the UK Biobank Resource under Application Number 67237.

Data collection and sharing for the Alzheimer's Disease Neuroimaging Initiative (ADNI) is funded by the National Institute on Aging (National Institutes of Health Grant U19 AG024904). The grantee organization is the Northern California Institute for Research and Education.

In the past, ADNI has also received funding from the National Institute of Biomedical Imaging and Bioengineering, the Canadian Institutes of Health Research, and private sector contributions through the Foundation for the National Institutes of Health (FNIH) including generous contributions from the following: AbbVie, Alzheimer's Association; Alzheimer's Drug Discovery Foundation; Araclon Biotech; BioClinica, Inc.; Biogen; Bristol-Myers Squibb Company; CereSpir, Inc.; Cogstate; Eisai Inc.; Elan Pharmaceuticals, Inc.; Eli Lilly and Company; EuroImmun; F. Hoffmann-La Roche Ltd and its affiliated company Genentech, Inc.; Fujirebio; GE Healthcare; IXICO Ltd.; Janssen Alzheimer Immunotherapy Research & Development, LLC.; Johnson & Johnson Pharmaceutical Research &Development LLC.; Lumosity; Lundbeck; Merck & Co., Inc.; Meso Scale Diagnostics, LLC.; NeuroRx Research; Neurotrack Technologies; Novartis Pharmaceuticals Corporation; Pfizer Inc.; Piramal Imaging; Servier; Takeda Pharmaceutical Company; and Transition Therapeutics.

AUTHOR CONTRIBUTIONS

E.T.W., M.L.E., A.R.K., A.C., T.E.M, and A.R.H. designed the research. E.T.W., M.L.E., A.R.K., W.C.A., T.J.A., N.C., S.H., D.I., T.R.M., S.R., K.S., R.T., B.S.W., A.C., T.E.M., and A.R.H performed the research. E.T.W., M.L.E., and A.R.K. analyzed data. E.T.W., M.L.E., A.R.K., A.C., T.E.M., and A.R.H. wrote the paper.

CONFLICT OF INTEREST

K. Sugden, A. Caspi, and T. E. Moffitt are listed as inventors of DunedinPACE, a Duke University and University of Otago invention licensed to TruDiagnostic for commercial uses; however, the DunedinPACE algorithm is open access for research purposes. All other authors report no conflict of interest.